J. Membrane Biol. 102, 141–152 (1988)

The Journal of
Membrane Biology

Slow Kinetics of a Potassium Channel in *Acetabularia*

A. Bertl, H.G. Klieber, and D. Gradmann
Plant Physiology Institute and Botanical Garden, D-3400 Göttingen, West Germany

Summary. The contribution of the major K^+ channel to the slow electrodynamic properties of the *Acetabularia* membrane has been investigated by patch-clamp techniques in the cell-attached mode using physiologically intact protoplasmic drops. This study comprises recording and statistical analysis of opening and closing events over long periods of time at various membrane voltages V_m, as well as measurement and evaluation of individual or averaged current responses of single channels upon large voltage steps. Although detailed observations reveal a variety of different states (such as bursts or various levels of conductance or noise), a serial three-state reaction kinetic model was adequate for the description of the channel properties which are relevant to the macroscopic electrical behavior. This model consists of an open state (o) and two closed states (1 and 2) with the approximate rate constants $k_{o1} = 1\ \text{sec}^{-1}$, $k_{1o} = 1\ \text{sec}^{-1}$, $k_{12} = 20 \cdot \exp(-V_m e/2kT)\ \text{sec}^{-1}$ and $k_{21} = 4 \cdot \exp(V_m e/2kT)\ \text{sec}^{-1}$. The current-voltage relationship of the open channel and the equilibrium k_{o1}/k_{1o} are relatively constant, whereas the (voltage-dependent) equilibrium k_{12}/k_{21} can spontaneously change within an order of magnitude at constant voltage.

Key Words *Acetabularia* · patch clamp · potassium channel · relaxation analysis · channel kinetics · channel statistics · reaction kinetic model

Introduction

Among the striking electrical properties of the plasmalemma of the giant, green marine alga *Acetabularia* (Gradmann, 1975), there are time constants in the range of seconds. There are two major systems of ion transport which are possible candidates responsible for these slow electric processes: a primary Cl^--ATPase (for review *see* Gradmann, 1984) and potassium-selective channels (Bertl & Gradmann, 1987). While earlier work has focused on the electrodynamic properties of the pump (Gradmann, 1975; Tittor, Hansen & Gradmann, 1983), the role of the K^+ channels is investigated here.

In a recent patch-clamp study (Bertl & Gradmann, 1987), the basic shape of the macroscopic steady-state current-voltage relationship of the passive ion pathways has already been assigned to a voltage-gated K^+ channel. The gating reaction has been described by a reaction kinetic model with three states in series: an open one and two closed ones, where only the equilibrium between the two closed states is voltage-dependent.

The present results are used to exclude alternatives to this model and to specify its two equilibria by estimates of the corresponding four rate constants. In addition, the model was tested for its ability to describe the observed slow current responses. For the sake of simplicity, actual series of short openings and even shorter closures were forced here by low-pass filtering (100 Hz) to appear as continuous openings. This simplification provides an apparently consistent approach, although for a correct treatment of the slow phenomena, the fast events must not be simply ignored (Roux & Sauvê, 1985; Blatz & Magleby, 1986).

Materials and Methods

Preparation and Solutions

Protoplasmic droplets of *Acetabularia mediterranea* with a diameter of about 100 μm were prepared as previously described (Bertl & Gradmann, 1987). Possible disturbances from the electrogenic Cl^- pump were reduced by using a standard medium with little Cl^- (130 mM) compared to normal seawater (about 500 mM). The ionic composition of this medium was (in mM): 5.5 $CaCl_2$, 5.5 $MgCl_2$, 130 KCl, 1 NaCl buffered with 5 Tris/MES at pH 8. If not stated otherwise, this medium was used in the bath and in the patch pipette.

Electrical Recordings

The main components of the electrical apparatus for measuring and storage of channel currents were a patch-clamp device (List, LPC 7), a digital audio processor (PCM-501ES, Sony) modified to enable DC-recordings, a video recorder (VS 220 RC PS, Grundig) for storage, an 8-pole Bessel filter (902LPF, Frequency Devices) and a digital oscilloscope (336, Sony-Tektronix, or 2090-3

Nicolet) for on-line monitoring of the experiments, for some preliminary evaluations (e.g. averaging by TEK336), and for analog output of selected data to an x/y plotter.

The patch-clamp measurements reported here have been carried out in the cell-attached mode because, in this configuration the outer membrane of the protoplasmic droplets does reflect physiologically intact plasmalemma under the conditions used (Bertl & Gradmann, 1987). That study has also demonstrated that for the conditions used here the transmembrane voltage V_m of these preparations is close to the Nernst equilibrium of potassium, E_{K^+} is about −30 mV with 130 mM K^+ in the medium and about 400 mM K^+ inside. Voltage data are reported here as transmembrane voltages, $V_m = E_{K^+} - V_p$, where V_p is the voltage between pipette and bath.

For relaxation experiments, voltage steps from a function generator (Model 166, Wavetek) were fed into the patch-clamp device. Since the employed protoplasmic droplets were rather large (about 100 μm in diameter), it was not possible to compensate the capacitive currents at the onset of a voltage step by the analog circuitry of the patch-clamp device. This compensation was carried out by computer-aided analysis of digital data.

Data Processing

For numerical analysis, analog output data from the videotape recorder were entered in digital form into a desk computer. Two configurations were used: either an AD converter (Labmaster, Tecmar) to the computer or intermediate storage (and pretreatment of the data such as averaging) by a digital oscilloscope and subsequent transfer by an IEEE bus to the computer for final analysis.

Apart from marked exceptions, the currents presented here are differences between the actual currents and the "baseline," i.e. the current when no channel is open.

If not stated otherwise, the recordings were low-pass filtered for analysis at a corner frequency f_c of 100 Hz and sampled at a rate of 200 Hz. This filter setting provides a good resolution of the slow processes (range of seconds) but eliminates fast processes in the kHz range by time averaging.

For the detection of channel openings and the measurement of dwell times the digitized patch-clamp recordings were processed as proposed by Vivaudou, Singer and Walch (1986). Lifetime histograms were evaluated by an unweighted least-squares fit of exponential functions to the data (*cf.* Dionne & Leibowitz 1982).

Relaxation times were obtained from averaged current signals in response to voltage steps by iterative application of linear regression.

Results

Qualitative Observations

Effect of I^- versus Cl^-

In a previous study (Bertl & Gradmann, 1987) some kinetic data of this channel have already been reported. Those data were obtained when (130 mM) Cl^- was replaced by I^-. The results showed lifetimes of the open state in the msec range. The present study focuses on slow kinetics which were measured with (130 mM) Cl^- in the medium instead of I^-. The difference of the behavior of the channel in these two media is illustrated by Fig. 1. In KI, the channel switches more frequently as compared to KCl conditions. On the other hand, the current through the open channel appears to be independent of the presence of these anions. This independence applies for a wide voltage range, as shown by the current-voltage relationship (Fig. 5 below).

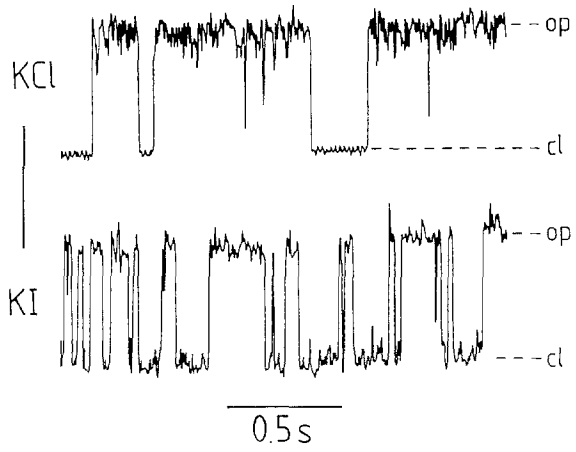

Fig. 1. Examples for different channel dynamics, dependent on the major anion in the medium; upper and lower trace identical conditions, except anions: upper trace 130 mM Cl^-, lower trace 130 mM I^-; V_m = +80 mV; vertical bar, 10 pA

Noise

In general, the "noise" of the open-channel currents is considerably larger than the noise of the baseline. In exceptional cases, however, this striking open-channel noise hardly shows up. The examples in Fig. 2 were recorded from the same patch at two different voltages. The entire recording (*not shown*) reveals the presence of two independent channels in the patch: one channel with only slightly increased noise compared to the baseline and another noisy one. Example tracings from each of these two channels are shown in Fig. 2. Since the current and its voltage dependence appear to be identical for both channels, these two channels are suggested to represent two different states of the same channel species. A more detailed inspection of Fig. 2 reveals a skew in the "scatter" of the noisy traces, which effectively results in slightly smaller steady-state (mean) currents of the open channel. The nature of the strong and asymmetric noise is elucidated by the following observations.

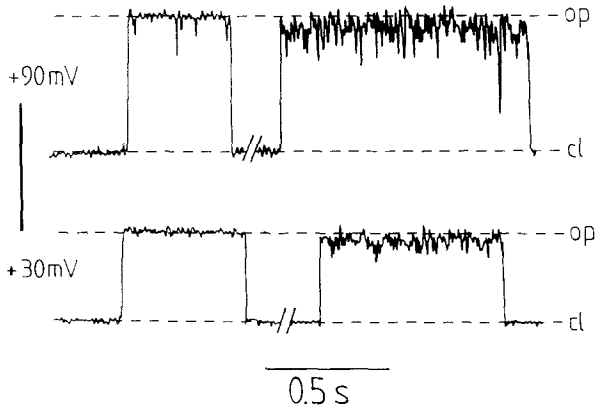

Fig. 2. Examples for different noise in open-channel current; recordings from the same patch at two voltages; similarities in open-channel currents at different voltages point to two different states (high noise and low noise) of the same type of channel; slight differences in mean open-channel currents (in high-noise channel about 10% smaller than in low-noise channel) point to (about 10%) interruptions during the apparent open time (in fact burst duration) of the noisy channel; vertical bar, 10 pA

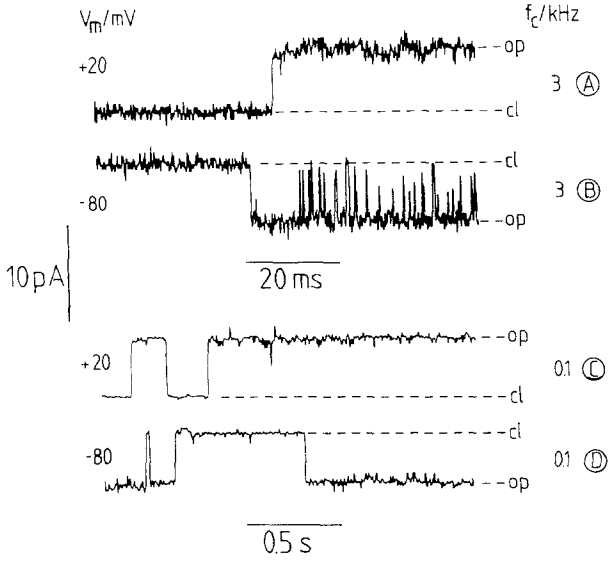

Fig. 3. Examples of the effect of the membrane voltage V_m and of low-pass filtering (f_c: corner frequency) on apparent open-channel dynamics; V_m = +20 mV (tracings *A* and *C*) and V_m = −80 mV (tracings *B* and *D*) reflect equal amounts of voltage displacement (50 mV) from equilibrium (−30 mV); high-frequency tracings (*A* and *B*) show voltage-dependent flickering, evident at −80 mV (*B*) and apparently absent at +20 mV (*A*); filtering with f_c = 100 Hz (tracings *C* and *B*) may convert actual series of short openings and closings (bursts or flickering, *B*) to apparent long-lasting open states

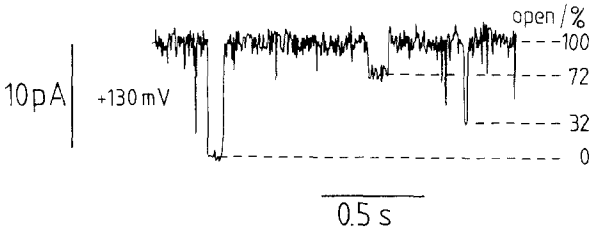

Fig. 4. Examples of intermediate current levels between open (100%) and closed (0%); apparent asymmetric noise of open-channel current at V_m = +130 mV

Bursts

Figure 3 shows channel currents at 100 Hz and at 3 kHz temporal resolution, at V_m = −80 mV and V_m = +20 mV, which corresponds to symmetrical voltage displacements by ±50 mV from E_{K^+}. At negative V_m (−80 mV), the long-lasting channel openings (as judged after 100 Hz low-pass filtering) are in fact interrupted by short and complete closures. This means that a long-lasting, noisy opening actually consists of a series of shorter openings separated by very short closures (burst). It can be estimated that the mean duration of these short interruptions is in the range of some 100 μsec and that during a burst the channel is closed about 10% of the time ($p_{cb} \approx 0.1$, p_{cb} being the probability of closure during a burst). This estimate of p_{cb} can be based on direct observations with high temporal resolution but also by a comparison of the steady-state open-channel currents. Moderate low-pass filtering will cause an asymmetric distribution of the open-channel currents with a tail towards zero. Stronger low-pass filtering will result in smaller ($1 - p_{cb}$) values for the current of the open state with increasingly smaller and more symmetric noise. Thus, continuous openings can be distinguished from bursts by an elevated steady-state current level (*see also* Fig. 2).

At V_m = +20 mV there is only little (symmetric) open-channel noise. Here, observation with 3 kHz bandwidths does not reveal flickering. It may, however, well exist beyond the actual limit of temporal resolution, since at more positive V_m, open-channel flickering can be observed again at a bandwidth of 3 kHz (*not shown*). The asymmetric open channel noise in Fig. 4 is the result of low-pass filtering of this flickering.

Partial Openings

The example tracing in Fig. 4 shows partial closings to two different intermediate current levels, which were occupied for many sampling intervals and could thus clearly be distinguished from brief spikes

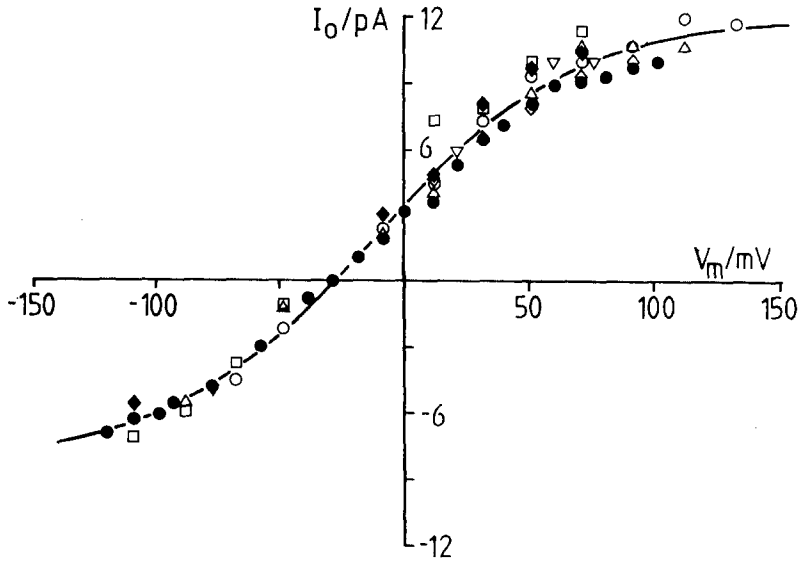

Fig. 5. Current-voltage relationship of the open channel; data (points) from seven different experiments, each represented with a separate symbol; open: 130 mM KCl, filled: 130 mM KI (*see* Fig. 1); curve fitted to all data by Eq. (6) with parameters (in 10^6 sec^{-1}) α^0: 154; β^0: 67; γ: 78; and δ: 54

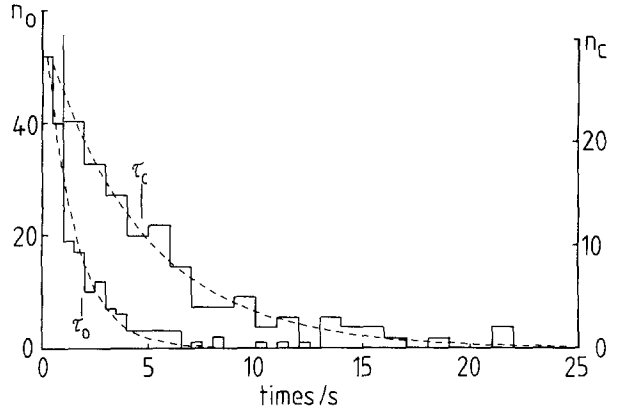

Fig. 6. Experimental frequency density histograms (discrete levels) and fitted probability density function (smooth curve) of open (left, 0.5-sec bins) and closed (right, 1.0-sec bins) times: one channel in patch, V_m: 40 mV, f_c: 100 Hz, sampling rate: 200 Hz; total time of observation: 1.5 ksec, total number of events: 184; fitted curves: τ_o = 1.8 sec from all events; τ_c = 4.6 sec without 55 events in first bin

which are due to low-pass filtering of short complete openings/closures. Such incomplete openings/closures can be detected most easily at $V_m \gg 0$ (*see* Fig. 3) where the frequency of events is high; however, they can also be observed at negative voltages.

Quantitative Evaluation of Slow Events

Steady State

The macroscopic (steady-state) current I_m through a particular channel is

$$I_m = I_o \cdot p_o \qquad (1)$$

where both the current I_o through the open channel and the open probability p_o may be voltage and time dependent. The voltage dependence of the current through the open channel $I_o(V_m)$ is illustrated by Fig. 5. Experiments from different patches yield very similar curves. Even substitution of Cl^- by I^- has no apparent effect on $I_o(V_m)$, although these conditions clearly affect the channel (by changing the switching frequency, *cf.* Fig. 1). In contrast, p_o and its voltage dependence varies considerably from one experiment to another. Even spontaneous fluctuations in p_o can be observed (*see* Fig. 9 below).

As a result of an observation of a single channel over 1.5 ksec, the lifetime histograms of openings and closures are shown by Fig. 6. Due to the extremely long apparent lifetimes, there is only a small number of events during long periods of observation. Therefore, and because of the fluctuations in p_o (*see also below*), the statistical significance of these data is limited. Fitting simple probability density functions (with one exponential only) to these data, resulted in fair compatibility which could not significantly be improved by introduction of another exponential component. It should be recalled, however, that the distribution of an unlimited number of observations will deviate from this simple pattern, for instance, due to the existence of slow fluctuations of the open probability (*see* Fig. 9) or due to the ignored flickering.

Fits, such as illustrated in Fig. 6, were carried out at different V_m (10, 40 and 70 mV). The results are summarized in Fig. 7. The apparent mean life-

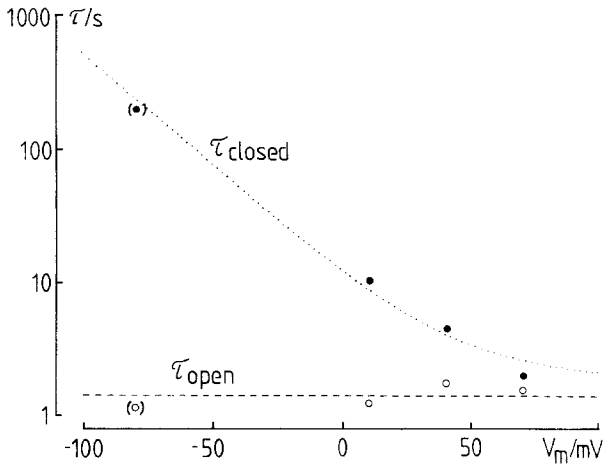

Fig. 7. Apparent state lifetimes versus V_m; data for 10, 40 and 70 mV same experiment as in Fig. 6, open time τ_o at −80 mV (1.2 sec) from experiment in Fig. 10 (average), closed time τ_c at −80 mV (193 sec): calculated by Eqs. (2a) and (7) with τ_o = 1.2 sec, and the average K_1 = 1.6 and K_2^0 = 4; dashed line: voltage-independent mean of open time; dotted curve: expectation for the large time constant t_{c2} from Eqs. (17a,b) with rounded values of k_{1o} = 0.5 sec^{-1}, k_{12}^0 = 20 sec^{-1}, k_{21}^0 = 4 sec^{-1}

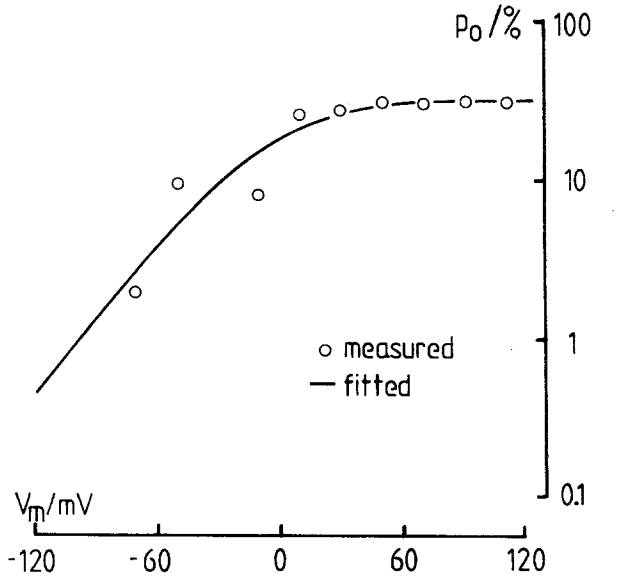

Fig. 8. Example of open probability p_o as a function of the membrane voltage V_m; semilogarithmic plot; curve fitted by Eq. (7a) with K_1 = 2.0 and K_2^0 = 1.1, approaching K_1 for $V_m \gg 0$ and Nernst slope (factor 0.1 per −58 mV) for $V_m \ll 0$

times τ_o and τ_c of the open and the closed state(s) are very large. Furthermore, the apparent mean lifetime of the open state appears to be rather independent of V_m, whereas the apparent mean lifetime of the closed state(s) τ_c increases from positive to negative V_m. The dotted curve in Fig. 7 is a subject of the Discussion.

The fitted parameters τ_o and τ_c and their voltage-dependence (Fig. 7) can be used to calculate a mean open probability

$$p_o = \tau_o/(\tau_o + \tau_c) \tag{2a}$$

and the voltage-sensitivity $p_o(V_m)$ of p_o. On the other hand, from the total open time T_o and the total closed time T_c the fractional open time

$$p_o' = T_o/(T_o + T_c) \tag{2b}$$

can be determined, which corresponds to the mean open probability p_o. The changes in p_o can be traced (even from preparations with multiple channels in the patch) by averaging the current over a given period of time. Such averages from time intervals between 30 and 1500 sec were available to determine p_o and its voltage dependence. The results comprise for $V_m \gg 0$ a saturation of p_o at about 0.5 which was well reproducible. For more negative V_m, the experimental values of p_o are increasingly scattered until they finally approach zero. This final decline can be approximated by a Nernstein exponential (factor 0.1 per −58 mV). One example out of five experiments is shown by Fig. 8 with a curve fitted to the data (Discussion). Similar data from all five experiments ranged from p_o = 0.001 at −110 mV to p_o = 0.5 at +130 mV.

Fluctuations

Over longer periods of observation the channel activity seems to fluctuate. An example is illustrated by Fig. 9(*A*) (same experiment as Fig. 6). There is the question as to whether these apparent changes in channel activity are statistical fluctuations of p_o as an intrinsic function (Eq. 3) of τ_o, τ_c and a given time interval Δt of observation, or whether these fluctuations point to an extra process of slow activation/inactivation.

If Δt is chosen to be much larger than $\tau_o + \tau_c$ the fractional open time (p_o', *cf.* Eq. 2b) becomes normally distributed with the same mean as p_o (Eq. 2a) and the standard deviation

$$\mathrm{SD}(p_o') = \frac{\tau_o \tau_c}{(\tau_o + \tau_c)^2}\left[\frac{2(\tau_o + \tau_c)}{\Delta t}\right]^{1/2}. \tag{3}$$

This is a result (*calculation not shown*) of using the method of statistical differentials (*cf.* Kempthorne & Folks, 1971).

For a Δt = 83 sec and with τ_o = 1.8 sec and τ_c = 4.6 sec (from Fig. 6), Eq. (3) yields for these conditions, $\Delta t \gg (\tau_o + \tau_c)$, a theoretical expectation

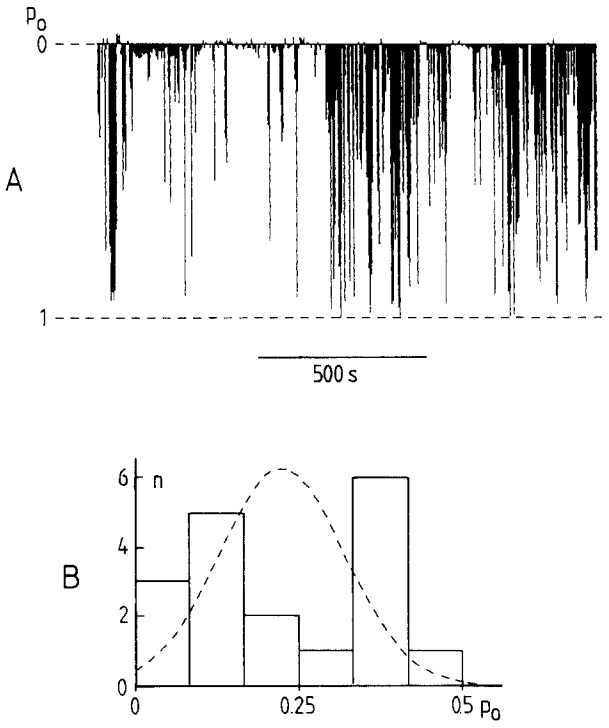

Fig. 9. Example for fluctuations in channel activity; same experiment as for Fig. 6. (*A*) Condensed representation of channel activity within the entire 1.5-ksec observation, every bar represents the mean current, $\bar{i}$ of a 4-sec period (left scale); since there is no baseline drift and the current level i_o of the open state is known, $\bar{i}$ is a measure of the mean open probability, $p_o = \bar{i}/i_o$, within the period of observation. This mean open probability is 22% for the entire 1.5 ksec. The inhomogeneous fluctuation pattern may be due to spontaneous nonstationary gating behavior. (*B*) Comparison of actual and theoretical frequency distribution of open probabilities, columns: experimental results from eighteen consecutive intervals à Δt = 83 sec of Fig. 9(*A*); curve: Gaussian distribution calculated with a mean p_o value of 0.22 and SD(p_o') of 0.077 (Eq. 3 with τ_o = 1.8 sec, τ_c = 4.6 sec and Δt = 83 sec)

range, SD(p_o') = 0.077 as illustrated by the curve in Fig. 9(*B*). However, the wide (double-peaked) distribution of p_o in this experiment (bars in Fig. 9*B*) as determined by eighteen nonoverlapping intervals of Δt, clearly deviates from the Gaussian distribution (curve in Fig. 9*B*) calculated with the mean value of about 22% and the theoretical SD(p_o') of about 8%. The physical meaning of this discrepancy is the presence of very slow fluctuations in channel activity (in the range of some 100 sec). These fluctuations do not simply reflect the physiological decay of the preparation, since both, decrease and increase of channel activity are observed (Fig. 9*A*).

Step Response

The voltage-dependence $p_o(V_m)$ of channel opening is shown by Figs. 7 and 8. The temporal behavior is

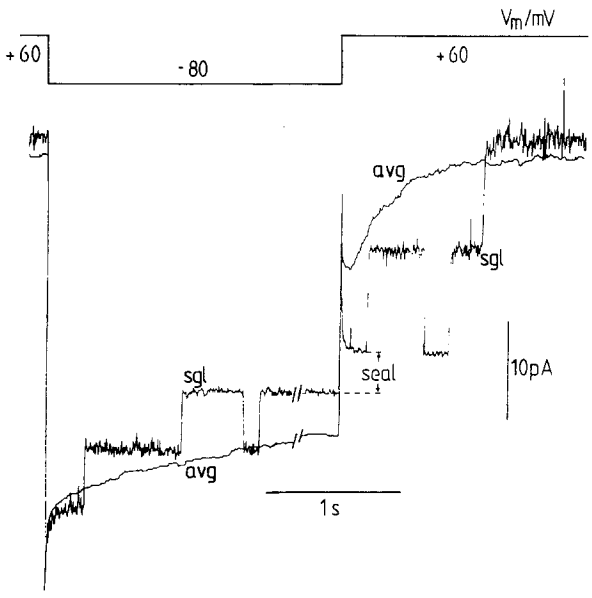

Fig. 10. Example (sgl) and average (avg, over 64 consecutive observations) of closing (left) and opening (right) kinetics of three individual channels upon steps of V_m between +60 and −80 mV; "seal" marks offset of baseline current due to a seal resistance of about 50 GΩ

illustrated by Fig. 10 for the current response upon large voltage steps of either sign between −80 mV (small p_o) and +60 mV where p_o is large (Fig. 8). The left part of Fig. 10 represents transitions from high to low p_o, i.e. inactivation, and the right part transitions from low to high p_o, i.e. activation. Both parts show an individual recording from a patch with three channels. Superimposed on the individual recordings are the corresponding averages from 64 consecutive runs.

At the beginning of the recordings upon a voltage step there is a capacitive artifact which could not be compensated by the apparatus. It was not possible to subtract a symmetric offset (sum of two exponentials) from these curves to obtain corrected tracings, which could adequately be described by a single exponential each. It was possible, however, to fit an offset to yield (after correction) only one exponential component in the averaged channel response at negative voltages, where the effect of a fast component of the channel is expected to be small compared to positive voltages (*see below*). This offset was subtracted (with the corresponding sign) from the two average curves in order to test whether an extra kinetic component is hidden in the relaxation at V_m = 60 mV (right part in Fig. 10) behind the initial artifact.

The results after correction are illustrated by Fig. 11. An initial lag in the current response is only visible in tracing (*A*). Superimposed on the two data sets are the two fitted exponentials. In tracing (*B*), it

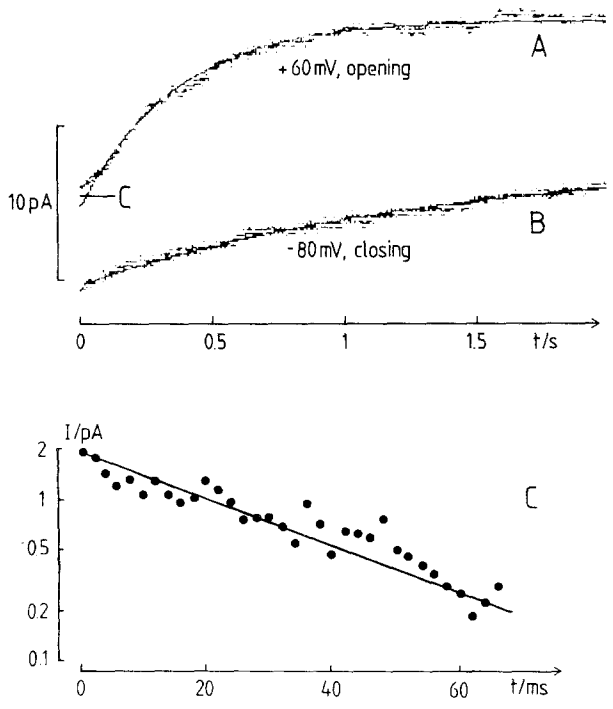

Fig. 11. Average tracings from Fig. 10 after subtraction of capacitive artifact [15 · exp(−*t*/22 msec) pA + 22.5 · exp(−*t*/4 msec) pA]. (*A*) Opening at +60 mV; (*B*) Closing at −80 mV; curves: fits with one exponential (*A*) (first 80 points omitted for fit): 12.9 · exp(−*t*/0.32 sec) pA, differing at the beginning by (*C*). (*B*) 8.3 · exp(−t/1.16 sec) pA, coinciding with data; all points used for fit. (*C*) Semilogarithmic plot of initial difference from (*A*) with fitted exponential: 1.8 · exp(−*t*/69.9 msec) pA

can hardly be distinguished from the experimental data. In tracing (*A*), the initial differences (*C*) between the data and the fitted exponential can be described by another exponential. These early differences and the corresponding second exponential fit are illustrated in a different scale by Fig. 11 (*C*).

Discussion

Qualitative Observations

From the examples in Figs. 1 to 4, various modes of the channel can be identified: long and short lifetimes of the open and closed states depending on whether Cl^- or I^- is present (Fig. 1), full conductance and at least two partial conductances (Fig. 4), high and low noise levels of the open channel (Fig. 2), different degrees of asymmetry of the open-channel noise, depending on the voltage (Fig. 3). Based on this collection of phenomena, which are peculiar to the channel, a great number of different states can be postulated.

Choice of the Model

On the other hand, for the reaction kinetic analysis of the present data simple models are desired which provide a satisfactory, quantitative description of the bulk data. For the sigmoid current-voltage curve of the open channel, a two-state model (Class-I kinetics, *cf.* Hansen et al., 1981) has turned out to be adequate (*cf.* Eq. 6, and Fig. 5). Apart from this two-state model for the steady-state current-voltage curve of the open channel, a minimum three-state model for gating (Eq. 7) is used here which has previously been introduced for the description of the stationary effective current-voltage curve of the channel (Bertl & Gradmann, 1987). This model consists of a linear reaction scheme with three states and four rate constants:

$$\text{open} \underset{k_{1o}}{\overset{k_{o1}}{\rightleftharpoons}} \text{closed}_1 \underset{k_{21}}{\overset{k_{12}}{\rightleftharpoons}} \text{closed}_2. \qquad [1]$$

The equilibrium constant $K_1 = k_{o1}/k_{1o}$ has been suggested to be voltage independent in contrast to the equilibrium constant $K_2 = k_{12}/k_{21}$ between the two closed states, for which a symmetric Eyring barrier is assumed with

$$k_{12} = k_{12}^0/U_c \quad \text{and} \quad k_{21} = k_{21}^0 \cdot U_c \qquad (4a,b)$$

where k_{12}^0 and k_{21}^0 are k_{12} and k_{21}, respectively, at zero voltage and $U_c = \exp(V_m z_g e/2kT)$ with a charge number $z_g = 1$ for gating.

The simplest model for voltage gating comprises voltage-dependent transitions between two states only, an open state and (only) one closed state. In this case, the open probability $p_o(V_m)$ should approach an upper limit of unity (channel always open) for large voltages (of appropriate sign). However, the experimental data (p_o in Fig. 8 and $1/K_1$ in Table 1) show a significantly smaller limit (about 50%). By this property, the existence of a second closed state can be concluded, and the voltage sensitivity of the system has to be located in this equilibrium between the two closed states. Physically speaking, in this model [1] the two states "open" and "closed$_1$" are occupied by about 50% each at large negative voltages, when state "closed$_2$" becomes zero; and *vice versa*, large positive voltages push the transporter into state "closed$_2$", while the states "open" and "closed$_1$" become depleted.

In general, the 3-state model would comprise a third pair of rate constants (k_{o2} and k_{2o}). However, the simpler version with $k_{o2} = k_{2o} = 0$ seems to be sufficient for our purpose.

While an alternative 3-state model (central open state between two closed states with one of the two

Table 1. Fits of K_1 and K_2^0 in Eq. (7a) to five experimental sets of $p_o(V_m)$ data; error: mean percent deviation between measured and fitted data

Exp. no.	K_1	K_2^0	error
1	1.33	5.00	35
2	1.73	2.10	52
3	1.81	7.51	13
4	2.04	1.10	14
5	1.13	5.85	4
mean	1.67	4.13	
SD	±0.37	±3.02	

equilibrium constants being voltage sensitive) is possible on grounds of the steady-state data, this alternative model will be excluded by dynamic aspects below.

Steady State

The macroscopic (steady-state) current-voltage relationship of the model is given by introducing voltage-sensitivity into Eq. (1):

$$I_m(V_m) = I_o(V_m) \cdot p_o(V_m) \tag{5}$$

where $I_o(V_m)$ is the current-voltage relationship of the open channel,

$$I_o(V_m) = z_o e \frac{\alpha\gamma - \beta\delta}{\alpha + \beta + \gamma + \delta} \tag{6}$$

where α, β, γ and δ are the rate constants of a cyclic two-state model for the transport of z_o elementary charges (*cf.* Hansen et al., 1981); the voltage sensitivity is in $\alpha = \alpha^0 \cdot U_o$ and $\beta = \beta^0/U_o$, α^0 and β^0 being α and β at zero voltage with $U_o = \exp(V_m z_o e/2kT)$; here the index "$o$" denotes the open channel current; the voltage-insensitive part of the reaction system is summarized by a pair of voltage-independent rate constants γ and δ. In Eq. (5), $p_o(V_m)$ is the voltage-dependent open probability

$$p_o(V_m) = \frac{1}{1 + K_1(1 + K_2)} = \frac{k_{21}k_{1o}}{k_{21}k_{1o} + k_{21}k_{o1} + k_{o1}k_{12}} \tag{7a,b}$$

with the voltage dependence in $K_2 = K_2^0/U_c^2$ (Eq. 7a), respectively, in k_{12} and k_{21} (Eq. 7b, *see* Eq. 4).

In a previous study (Bertl & Gradmann, 1987) p_o was fitted by Eq. (7a) with three variables (K_1, K_2^0 and z_g). In this study, more data are available and fits with a constant $z_g = 1$ yield good descriptions as well (*see* Fig. 8). The results from five experiments are listed in Table 1. These data indicate that the striking instability of p_o is due to changes in K_2^0 rather than in K_1. In other words, the saturation of p_o at $V_m \gg 0$ is relatively constant around 0.5 and the onset of the exponential decline of p_o with (negative) V_m may vary considerably even between consecutive observations of an individual channel under apparently constant conditions. There may be regulatory reactions (*cf.* Hansen, 1980) located in the kinetic vicinity of the closed compound state which were not under control in these experiments.

Dynamics

The aim of the dynamic analysis is to determine absolute values of the four rate constants of the reaction scheme [1]. For this purpose a macroscopic as well as a microscopic treatment of the problem can be carried out. The latter treatment is a statistical analysis of open and closed times of an individual channel. For the former treatment, macroscopic current relaxations upon voltage steps can be used. Here, an attempt of the macroscopic treatment is carried out and its predictions on microscopic observations are compared with the corresponding measurements.

Relaxation Analysis

Theory. The dynamic properties of the gating reaction scheme [1] can be described by the set of three differential equations

$$-p_o/\tau = dp_o/dt = -k_{o1}p_o + k_{1o}p_1 \tag{8a}$$

$$-p_1/\tau = dp_1/dt = k_{o1}p_o - (k_{1o} + k_{12})p_1 + k_{21}p_2 \tag{8b}$$

$$-p_2/\tau = dp_2/dt = k_{12}p_1 - k_{21}p_2. \tag{8c}$$

In general, the macroscopic current response $I_m(t)$ consists of a steady-state component I_0 as calculated by Eqs. (6) and (11a), and a transient comprising two exponentially decaying components:

$$I_m(t) = I_0 + I_1 \exp(-t/\tau_1) + I_2 \exp(-t/\tau_2). \tag{9}$$

The two relaxation time constants τ_1 and τ_2 are given by

$$1/\tau_{1,2} = 0.5a + 0.5 \cdot (a^2 - 4b)^{1/2} \tag{10a,b}$$

with the auxiliary variables

$$a = k_{o1} + k_{1o} + k_{12} + k_{21} = 1/\tau_1 + 1/\tau_2 \tag{10c}$$

and

$$b = k_{o1}k_{12} + k_{o1}k_{21} + k_{1o}k_{21} = (1/\tau_1)(1/\tau_2). \quad (10d)$$

For the calculation of the amplitudes I_1 and I_2 in Eq. (9), the steady-state changes of the probability Δp before ($t = 0$) and after ($t = \infty$) the step are used from the open state,

$$\Delta p_o = p_o(t = 0) - p_o(t = \infty) \quad (11a)$$

(*compare* Eqs. 7, 16b) and from state$_1$

$$\Delta p_1 = p_1(t = 0) - p_1(t = \infty) \quad (11b)$$

with

$$p_1 = \frac{k_{21}k_{o1}}{k_{o1}k_{12} + k_{o1}k_{21} + k_{21}k_{1o}}. \quad (11c)$$

For τ_1 and τ_2, Eq. (8a) yields the ratio

$$P_{o1}/P_{11} = k_{1o}/(k_{o1} - 1/\tau_1) \quad (12a)$$

and

$$P_{o2}/P_{12} = k_{1o}/(k_{o1} - 1/\tau_2) \quad (12b)$$

where the first index to P denotes the state and the second one the time constant. These four portions (P_{o1}, P_{11}, P_{o2} and P_{12}) can be calculated by the four Eqs. (12a), (12b), (13a) and (13b) with

$$\Delta p_o = P_{o1} + P_{o2} \quad \text{and} \quad \Delta p_1 = P_{11} + P_{12}. \quad (13a,b)$$

Thus the amplitudes I_1 and I_2 of the two exponentials (Eq. 9) are

$$I_1 = I_o P_{o1} \quad \text{and} \quad I_2 = I_o P_{o2} \quad (14a,b)$$

with

$$P_{o1} = \frac{\Delta p_o(k_{o1} - 1/\tau_2) - \Delta p_1 k_{1o}}{1/\tau_1 - 1/\tau_2} \quad (14c)$$

and

$$P_{o2} = \frac{\Delta p_o(k_{o1} - 1/\tau_1) - \Delta p_1 k_{1o}}{1/\tau_2 - 1/\tau_1}. \quad (14d)$$

For the sake of completeness and for further discussion below, the corresponding partial amplitudes of state$_1$ are given as well:

$$P_{11} = \frac{(1/\tau_1 - k_{o1})[\Delta p_o(1/\tau_2 - k_{o1}) + \Delta p_1 k_{1o}]}{k_{1o}(1/\tau_1 - 1/\tau_2)} \quad (14e)$$

Table 2. Comparison of measured (rounded) data and calculated ones by the reaction scheme [1] with the parameters $k_{o1} = 1.08$ sec^{-1}, $k_{1o} = 1.11$ sec^{-1}, $k^0_{12} = 18.96$ sec^{-1}, $k^0_{21} = 3.80$ sec^{-1}

Parameter	Value		Source
	measured	calculated	
$\tau_1(+60)$/sec	0.050	0.053	fast relax. at $V_m = +60$ mV
$\tau_1(-80)$/sec	—	0.010	fast relax. at $V_m = -80$ mV
$\tau_2(+60)$/sec	0.05	0.56	slow relax. at $V_m = +60$ mV
$\tau_2(-80)$/sec	1.00	0.93	slow relax. at $V_m = -80$ mV
$A_1/A_2(+60)$	−0.100	−0.096	amplit. ratio at $V_m = +60$ mV
$A_1/A_2(-80)$	—	−0.010	amplit. ratio at $V_m = -80$ mV
$K_1 = k_{o1}/k_{1o}$	1.00	0.97	satur. p_o at $V_m \gg 0$: ≈0.5
$K^0_2 = k^0_{12}/k^0_{21}$	5.0	4.99	fit of Eq. (7a) to $p_o(V_m)$, *see* Fig. 7

$$P_{12} = \frac{(1/\tau_2 - k_{o1})[\Delta p_o(1/\tau_1 - k_{o1}) + \Delta p_1 k_{1o}]}{k_{1o}(1/\tau_2 - 1/\tau_1)}. \quad (14f)$$

Parameter Identification. The desired four parameters (k_{1o}, k_{o1}, k^0_{12} and k^0_{21}) have been fitted to satisfy the (rounded) six experimental parameters as listed in Table 2. The direct numerical results yield slightly worse fits, because of the τ_2 values which appear more different in the results (*see* Fig. 11). On the other hand, the statistical variation of the results may justify the rounded values as a crude but realistic approach.

Consequences. The model with the fitted rate constants does not only allow the numerical reproduction of the measurements. It also enables the calculation of additional intrinsic features of the model, such as the fast exponential relaxation at −80 mV, which was not detected in the experiments. The corresponding expectation values are listed in Table 2 as well. They show a time constant, $\tau_1(-80)$, and an amplitude ratio, $A_1/A_2(-80)$, which are actually too small as to be detected in the experiments (Fig. 11*A*).

In the model, the voltage dependence of the short relaxation time τ_1 is such that τ_1 is maximum when the sum $k_{12} + k_{21}$ of the voltage-dependent rate constants is minimum. For $K^0_2 \approx 5$, this condition is met at V_m of about +40 mV, when k_{12} equals k_{21} (*cf.* Eq. 4). For larger voltage displacements from +40 mV, τ_1 becomes very small.

The fitted rate constants render the voltage-dependent equilibrium between the two closed states relatively rapid: $k_{12} + k_{21} \gg k_{1o} + k_{o1}$. Under these conditions, the voltage dependence of the long relaxation time τ_2 is such that for $V_m \ll 0$, τ_2 ap-

proaches the limit of $1/k_{1o}$, and for $V_m \gg 0$ the limit of $1/(k_{1o} + k_{o1})$.

With these conditions, $k_{12} + k_{21} \gg k_{1o} + k_{o1}$, the minimum model for our data could be reduced from four to three parameters, namely the two slow and voltage-independent rate constants k_{o1} and k_{1o} plus a fast and voltage-dependent equilibrium K_2. With this simplification of the model, there is only one exponential component expected in the relaxations (τ_2) or in the lifetime distributions (t_{c2}, *see below*). With respect to the actual accuracy of the measurements, this simpler model, where the two preliminary rate constants k_{12}^0 and k_{21}^0 are replaced by one equilibrium constant K_2^0, essentially satisfies the data as well, without affecting the main conclusions.

Discrimination of Alternative Models. The voltage-dependence of τ_2 can also be used to exclude an alternate model with slow (still voltage-dependent) equilibrium of the two closed states and frequent (still voltage-insensitive) transitions between the open state and state closed$_1$ ($k_{1o} + k_{o1} \gg k_{12}^0 + k_{21}^0$). The slow relaxation time τ_2 of this alternate model is maximum when $k_{12} = k_{21}$ (i.e., at about +40 mV for $K_2^0 \approx 5$) and declines with increasing voltage displacements of either sign. Since in the performed step response experiments the used −80 mV means a large displacement (−120 mV) from this voltage compared to the used +60 mV (20-mV displacement only), this alternate model predicts a much smaller τ_2 at −80 mV than at +60 mV. The measurements discard this alternate model because τ_2 behaves the opposite way.

These relaxation properties allow also discrimination between the used gating model and the mentioned alternative 3-state model with a central open state. This can algebraically be demonstrated by exchanging the indices "*o*" and "1" in Eqs. (8), the corresponding treatment thereafter and respective use of Eqs. (14e,f). The result can briefly be illustrated in physical terms by following considerations. Upon a (voltage-induced) step from low p_o to high p_o, the alternative model will exhibit a peak in the time course $p_o(t)$ of p_o. Thus, the proportional current transient $I_o \cdot p_o(t)$ would look like a current transient across a capacitance (capacitive behavior). However, the investigated channel clearly shows inductive behavior (monotonic increase of I_t due to $p_o(t)$) under these conditions (main response in Fig. 10 right after capacitive artifact, and Fig. 11*B*). Vice versa, for steps from high to low p_o, the measurements and the chosen model show capacitive behavior (Fig. 10 left and Fig. 11*A*) and the alternative model would behave like an inductance.

In this context, a note may be added on the physical impact of the second closed state of the reaction kinetic model [1] on the electrodynamic properties of the system. The effect of voltage changes on voltage-dependent rate constants is assumed to be instantaneous. If there were only one open state and one closed state with voltage-dependent transitions, a voltage step should cause the immediate beginning of a current change with one exponential (Eq. 9 with $I_2 = 0$). However, if a delay is observed between the immediate change (I_0 in Eq. 9) and the main exponential one (*cf.* Fig. 11*A*), an additional state is required which causes an additional exponential component with an amplitude opposite to the amplitude of the main one and parallelism between the amounts of the new amplitude and the new time constant: a small delay corresponds to an additional exponential with a small time constant and a small amplitude. In physical terms, such a delay can be described by an additional low pass.

In conclusion, the kinetic properties of the K^+ channels are considered to be essential for the voltage-dependent electrodynamics of the *Acetabularia* membrane, at least within the investigated ranges of voltage (about −100 to +100 mV) and time (about 10 msec to 10 sec).

Microscopic Approach

The microscopic channel properties of the reaction system [1] is determined by the four rate constants k_{o1}, k_{1o}, k_{12}^0 and k_{21}^0, which also determine the transition probabilities between states. The following parameters can be calculated according to Colquhoun and Hawkes (1981). The mean lifetime of the open state t_o is

$$t_o = 1/k_{o1} \tag{15}$$

where k_{o1} can be understood as the decay constant for the open state. The probability density function for the open times $A_o(t)$ is

$$A_o(t) = (1/t_o) \exp(-t/t_o). \tag{16}$$

The lifetime distribution of the entity of the two closed states comprises two constants t_{c1} and t_{c2} with

$$1/t_{1,2} = 0.5 \cdot (k_{1o} + k_{12} + k_{21}) \pm 0.5 \cdot [(k_{1o} + k_{12} + k_{21})^2 - 4k_{21}k_{1o}]^{1/2}. \tag{17a,b}$$

The probability densities for the closed times $A_c(t)$ will be

$$A_c(t) = A_{c1} \exp(-t/t_{c1}) + A_{c2} \exp(-t/t_{c2}) \tag{18a}$$

Table 3. Voltage-dependent channel kinetics[a]

Parameter V_m/mV	t_o/sec	t_{c1}/sec	t_{c2}/sec	$A_{c1}t_{c1}$/%	$A_{c2}t_{c2}$/%
−110	0.93	0.006	350.2	0.66	99.3
−80	0.93	0.011	108.3	1.17	98.8
	1.2		193		
−50	0.93	0.019	34.0	2.02	98.0
−20	0.93	0.032	11.2	3.22	96.8
10	0.93	0.048	4.1	4.15	95.8
	1.3		10	≈0	≈100
40	0.93	0.057	1.9	3.40	96.6
	1.8		4.6	≈0	≈100
70	0.93	0.050	1.2	1.43	98.6
	1.6		2.0	≈0	≈100
100	0.93	0.033	1.0	0.35	99.7

[a] t_o: mean lifetime of open state; t_{c1} and t_{c2}: short and long time constant of lifetime distribution of combined closed states; $A_{c1}t_{c1}$ and $A_{c2}t_{c2}$: percentage portions of closed periods from short- and long-time component of the distribution; not underlined: calculations by Eqs. (15) to (18) with fitted parameters from relaxation experiments and analysis (Figs. 10 and 11, Table 2); underlined: measured single-channel kinetics, different experiment (in Fig. 7).

with

$$A_{c1} = k_{1o}(1/t_{c1} - k_{21})/(1/t_{c1} - 1/t_{c2}) \tag{18b}$$

and

$$A_{c2} = k_{1o}(1/t_{c2} - k_{21})/(1/t_{c1} - 1/t_{c2}). \tag{18c}$$

Values for the parameters t_o, t_{c1}, t_{c2}, and the percentage portions of $A_{c1}t_{c1}$ and $A_{c2}t_{c2}$ on the entire number (100%) of events observed, are calculated for several voltages by these equations with the model parameters in Table 2. The results are listed in Table 3 together with experimental data as far as available (from Fig. 7). There is fair coincidence between the main features of the predicted and experimental data: amount and voltage insensitivity of t_o as well as predominance and voltage sensitivity of the long-time component in the closed times distribution.

Furthermore, the calculated numbers in Table 3 show that the experimentally unidentified parameters (t_{c1} and $A_{c1}t_{c1}$) are, in fact, beyond the actual resolution of the experiments. These agreements provide confidence that the reaction kinetics of the investigated K^+ channel are adequately described by the scheme [1] with its approximate rate constants as listed in Table 2.

Despite this coincidence, it should be kept in mind that this model is the result of severe simplification. Using enhanced temporal resolution (instead of filtering with 100 Hz, *see* Fig. 3), reveals the long-lasting "apparent" open states to be frequently interrupted by short closures. This does not only render the genuine open time to be much smaller, it also causes an apparent excess of long-lasting opening events, compared to the predictions of the simple distribution with just one exponential component. Furthermore, the short interruptions will introduce an extra component in the closed-time distribution. The correct treatment of such details has already been worked out explicitly (Roux & Sauvê, 1985; Blatz & Magleby, 1986). However, the presented data are insufficient for a detailed analysis.

Outlook

These features as well as further details such as shown in Figs. 1 to 4, certainly require modification and/or expansion of the model. It is not yet clear, how many states and/or reactions must be added to the present model. For example, with $k_{o2} \approx 10^3$ sec and $k_{2o} \approx 10^2$ sec, open-channel flickering could fairly be simulated already. On the other hand, closing of the reaction cycle with $k_{o2}, k_{2o} > 0$, introduces severe consequences on the thermodynamic and kinetic properties (*cf.* Finkelstein & Peskin, 1984) which are not worked out yet for the channel under investigation, since kinetic analysis and modeling of the fast processes of the channel require further investigation.

This work was supported by the Deutsche Forschungsgemeinschaft (Gr 409/9-5,6).

References

Bertl, A., Gradmann, D. 1987. Current-voltage relationships of potassium channels in the plasmalemma of *Acetabularia*. *J. Membrane Biol.* **99**:41–49

Blatz, A.L., Magleby, K.L. 1986. Correcting single channel data for missed events. *Biophys. J.* **49**:967–980

Colquhoun, D., Hawkes, A.G. 1981. On the stochastic properties of single ion channels. *Proc. R. Soc. London B.* **211**:205–235

Dionne, V.E., Leibowitz, M.D. 1982. Acetylcholine receptor kinetics. A description from single-channel currents at snake neuromuscular junctions. *Biophys. J.* **39**:253–261

Finkelstein, A., Peskin, C.S. 1984. Some unexpected consequences of a simple physical mechanism for voltage-dependent gating in biological membranes. *Biophys. J.* **46**:549–558

Gradmann, D. 1975. Analog circuit of the *Acetabularia* membrane. *J. Membrane Biol.* **25**:183–208

Gradmann, D. 1984. Electrogenic Cl^- pump in the marine alga *Acetabularia*. *In:* Chloride Transport Coupling in Biological Membranes and Epithelia. G.A. Gerencser, editor. pp. 13–61. Elsevier Science, Amsterdam

Hansen, U.P. 1980. Homeostasis in *Nitella:* Adaptation of H^+-transport to the phostosynthetic load. *In:* Plant Membrane Transport: Current Conceptual Issues. R.M. Spanswick, W.J. Lucas, and J. Dainty, editors. pp. 587–588. Elsevier Science, Amsterdam

Hansen, U.P., Gradmann, D., Sanders, D., Slayman, C.L. 1981. Interpretation of current-voltage relationships for "active" ion transport systems: I. Steady-state reaction-kinetic analysis of class-I mechanisms. *J. Membrane Biol.* **63:**165–190

Kempthorne, O., Folks, L. 1971. Probability, Statistics and Data Analysis. Iowa State University Press, Ames, Iowa

Roux, B., Sauvê, R. 1985. A general solution to the time interval omission problem applied to single channel analysis. *Biophys. J.* **48:**149–158

Tittor, J., Hansen, U.P., Gradmann, D. 1983. Impedance of the electrogenic Cl^- pump in *Acetabularia:* Electrical frequency entrainements, voltage-sensitivity and reaction kinetic interpretation. *J. Membrane Biol.* **75:**129–139

Vivaudou, M.B., Singer, J.J., Walch, J.V. 1986. An automated technique for analysis of current transitions in multi level single channel recordings. *Pfluegers Arch.* **407:**355–364

Received 15 October 1987; revised 6 January 1988